Available online at www.sciencedirect.com

ScienceDirect

Energy Procedia 49 (2014) 538 – 550

Energy Procedia

SolarPACES 2013

Strategies enhancing efficiency of cavity receivers

R. Uhlig[a]*, R. Flesch[b], B. Gobereit[a], S. Giuliano[a], P. Liedke[a],

[a]*Institue of Solar Resarch, German Aerospace Center (DLR), Pfaffenwaldring 38-40, 70569 Stuttgart, Germany*
[b]*Institue of Solar Resarch, German Aerospace Center (DLR), Karl-Heinz-Beckurts-Str. 13, 52428 Jülich, Germany*

Abstract

Introducing solar energy into the gas turbine of Combined Cycle systems (CC) offers significant advantages over other solar power plant concepts. A promising way to introduce solar power is solar preheating of the compressor discharge air before it enters the combustor of the gas turbine using a receiver built consisting of several metallic tubes. The main challenge during the design of such a receiver is the low solar flux capability caused by the limited convective heat transfer. To ensure a sufficient efficiency, the receiver is usually located in a cavity. The heat losses by conduction through the (insulated) cavity walls can be reduced by increased insulation thickness. Heat losses by radiation and convection to ambient depend strongly on the aperture area, receiver inclination and the receiver temperature. The receiver temperatures can be reduced by increasing the cavity size, as the flux distribution gets more homogenous and the overall flux density is reduced. Following heat losses by radiation and convection to ambient are reduced. On the other hand additional costs for the cavity walls have to be considered. The paper deals with the comparison of two different strategies to increase the receiver efficiency of a cavity receiver used to heat the compressed air of a 4.7 MWel turbine from 330°C up to 800°C, with a mass flow of 15.9 kg/s at 10 bar_{abs}. The influence on the levelized cost of energy (LCOE) of different receiver sizes and one design option (transparent covering of aperture) for reducing the convections losses were analyzed and compared. The thermal and hydraulic layout was done for a thermal heat of 8.4MWth and 250 mbar pressure drop using thermal finite element (FE) models considering the local heat flux distribution, heat transfer to working fluid, radiation exchange between components and ambient as well as conduction and convection losses of the cavity. As the convective losses play a significant role, CFD models were used to evaluate the convective heat losses.

Selection and peer review by the scientific conference committee of SolarPACES 2013 under responsibility of PSE AG.
Final manuscript published as received without editorial corrections.

Keywords: Solar tower; Combined Cycle, Tubular receiver; Convection losses; Window

* Corresponding author. Tel.: +49 711 6862 554; fax: +49 711 6862 747.
E-mail address: ralf.uhlig@dlr.de

Selection and peer review by the scientific conference committee of SolarPACES 2013 under responsibility of PSE AG.
Final manuscript published as received without editorial corrections.
doi:10.1016/j.egypro.2014.03.058

1. Introduction

1.1. Solar Hybrid Systems

Introducing solar energy into the gas turbine of solar-hybrid combined cycle (SHCC®) offers significant advantages over other solar power plant concepts. A promising way to introduce solar power is solar preheating of the compressor discharge air before it enters the combustor of the gas turbine. A scheme of the concept is shown in Figure 1. In order to reach the required high temperatures, a high concentration of the solar radiation is necessary. This is achieved in a solar tower plant where a high number of movable mirrors ("heliostats") concentrate and aim the incoming solar radiation to a receiver on top of a tower, creating a focal spot with a diameter of only a few meters. The function of the receiver is the transfer of energy contained in the highly concentrated radiation to the heat transfer medium (pressurized air).

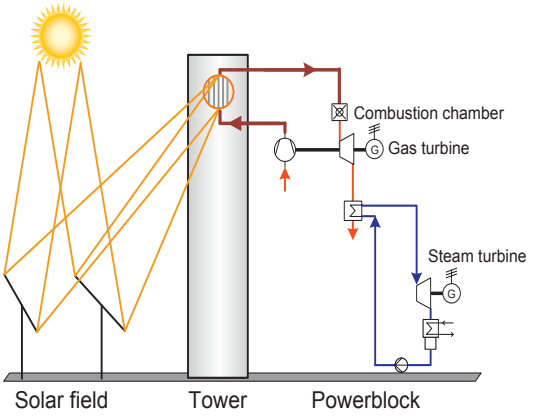

Fig. 1 Solar-hybrid Combined Cycle (SHCC®)

1.2. Receiver technology

The receiver is one key component of a solar tower system. For gas turbine systems, where air is the heat transfer fluid, the receiver design has to deal with a low heat transfer caused by the limited pressure drop of the gas turbine itself. Further high operating temperatures combined with inhomogeneous heat flux distribution on the receiver are obstacles preventing high receiver efficiency. Therefore such receivers are commonly located in a cavity where the heat losses are reduced by lowering the heat flux, resulting in lower temperatures on the absorber. Furthermore, the internal reflections inside the cavity lower the optical and infrared radiating losses. A common way to build such a receiver is the usage of metallic tubes. Within the SOLGATE project a tubular receiver was developed to heat up air from 290°C up to 500°C with a thermal power of 300kW [1]. A tubular receiver for a microturbine system was developed during the SOLHYCO project heating up air from 600 up to 800°C with a thermal power of 300kW [2]. Within the SOLUGAS project a tubular receiver heating up air from 330 up to 800°C with a thermal power of 3MW was developed [3].

2. Thermal modeling of a tubular cavity receiver

The presented receiver designs are designed to heat up the compressed air of a 3.9 MW_e turbine from 330°C up to 800°C with a mass flow of 15.9 kg/s at 10 bar_{abs}. with a maximum pressure drop of 250 mBar. The receiver inlet air is distributed and collected by tubular headers forming rings. The solar radiation is absorbed at the parallel absorber tubes arranged between the headers. The absorber tubes are located in an insulated cavity with an aperture diameter of 4m. The outer diameter of the cavity depends on the amount of used parallel tubes and the thickness of inner insulation.

2.1. Design

The allowable pressure drop of the turbine limits the possible mass flow within the absorber tubes, as pressure drop is strongly related to the fluid velocity. The required number of parallel connected absorber tubes is given by the inner diameter and the length of the tubes. From a thermodynamic point of view, small diameters and short tubes would be the best as the heat transfer ability is maximized.

Further small diameters need a small wall thickness (resistance against pressure) and lead therefore to lower thermal gradients and finally lower material costs. On the other hand a high number of parallel tubes increase the manufacturing costs (welding of absorber tubes to the headers and other components).

The presented concept foresees an individual thermal strain compensation using a metallic bellow at the inlet and a diffusor section (lower pressure drop) at the outlet for each absorber tube. Furthermore, costs must also be considered, and increase the more parallel tubes are used. To filter possible receiver designs an EXCEL®/MATLAB® based tool was used that considered manufacturing and material costs of the receiver as specific costs based on current prices of material and costs for several manufacturing steps (drilling holes, welding tubes, assembling). The main interest was to find the ideal receiver configuration (number of parallel absorber tubes and geometric dimensions of the components). Ideal in this case means that the thermo hydraulic needs are fulfilled at the lowest costs. To ensure this, heat transfer from the absorber tubes into the working fluid is modeled by discretizing the absorber tubes into a large number of segments along the flow direction resulting in a one-dimensional approximation. Heat transfer into the fluid is calculated using Gnielinski Nusselt correlations found in [4] at each discrete segment using temperature dependent fluid properties. In the same way the pressure drop at each segment is calculated using Reynolds-correlations from [4]. The wall thickness of the tubes and headers are determined by an empiric formula for pressure-vessels found in [5] and using material stresses for the given temperatures. Table 1 shows the results of two receiver designs with different receiver dimensions (V1=”small receiver”; V2=”large receiver”). The design V2 shows higher specific costs than V1, mainly caused by higher material costs (absorber tubes and cavity insulation). Fig. 2 gives an impression of the overall dimensions of the two receiver designs.

Table 1: Design results receiver

Design results	Receiver V1	ReceiverV2
Specific receiver costs (material and manufacturing) [€/kW$_{th}$]	135	225
number of parallel absorber tubes	200	270
inner diameter absorber tube [m]	0.025	0.025
outer diameter absorber tube [m]	0.03	0.03
radiated length of the absorber tubes [m]	6	10
cavity aperture area [m^2]	12.6	12.6
internal cavity area [m^2]	206.2	420.1
external cavity area [m^2]	239.5	466.6
average heat transfer coefficient [W/m^{2}K]	465	370

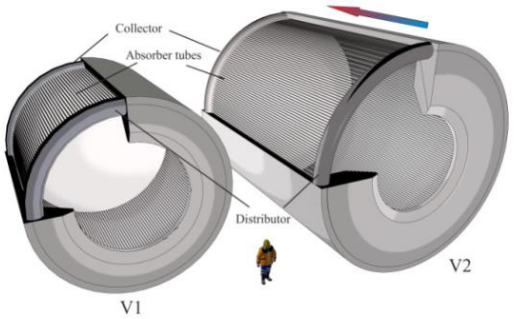

Fig. 2: Sketch receiver design V1 and V2

2.2. Thermal model

To evaluate the efficiency of the receiver, a thermal FE model was used. As the absorber tubes are located in a cavity, the radiation exchange between the tubes, cavity walls and ambient follow the rules of reflection and absorption. The model considers this using a ray-tracing based algorithm for the solar wavelength. The code uses the geometric data and the optical properties of each FE of the mesh to calculate the expected heat flux distribution considering direct absorption as well as grey diffuse solar radiation exchange.

The absorber is modeled with an absorptivity of 0.9 and the cavity with an absorptivity of 0.3. The heat transfer to working fluid is modeled using one- dimensional fluid-flow elements. They consider heat and mass transfer of the fluid using temperature dependent fluid properties and a heat transfer coefficient. At the infrared wavelength the radiation exchange is modeled using the radiosity method of the FE code. The heat losses by convection to ambient are considered using a heat transfer coefficient and the ambient temperature as bulk temperature estimated using a Nusselt correlation at the inner area of the cavity. Finally the conduction losses through the insulated cavity are modeled as a heat flow at the outside walls of the cavity.

2.3. Results

Table 2 shows the results of the thermal model. At design point (P_DP/P=1) the smaller receiver (V1) reaches a receiver of efficiency of 75% while the larger receiver (V2) reaches an efficiency of 80%. The reason for the lower efficiency of design V1 is the higher material temperature due to the higher heat fluxes inside the cavity resulting in higher radiation and convection losses for this design. Furthermore the optical losses of the V1 design are higher as the cavity effect is smaller than for design V2. The conduction losses do not play a significant role. It is seen that at the receiver efficiency is lower during part load situations (P_DP/P<1) (Fig. 3).

Table 2: Results thermal model

	Receiver V1	ReceiverV2
Receiver optical efficiency	0.94	0.97
Receiver thermal efficiency	0.80	0.83
Receiver total efficiency	0.75	0.80
Maximum absorber temperature [C°]	1030	895
Maximum cavity temperature [C°]	1190	1013

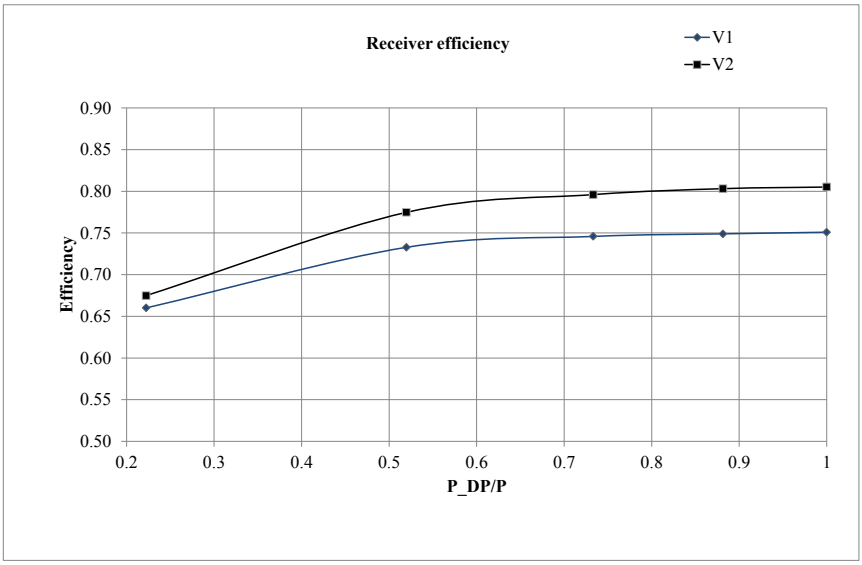

Fig. 3 Total receiver efficiencies

3. Convection losses

3.1. Introduction

The convection in the receiver is driven by density gradients in the fluid of the cavity from high temperature gradients between the ambient and receiver temperature. Therefore cold air entering the receiver at the bottom of the aperture area is heated up by the hot walls. This air leaves at the top of the aperture. Due to the influence on the receiver efficiency, the convective losses were the focus of several studies. As air flows in a cavity are very complex, it is not possible to give an analytic solution for the convective losses for all receiver designs, sizes and situations (eg. wind). Hence, first analysis proposed to use a correlation for a vertical flat plate with the size of the aperture opening [18] or to calculate the heat losses of the inner cavity surface by using adequate correlations [17]. The first analysis taking the flow phenomena in a cavity receiver into account was performed by Eyler [8]. He used a 2D numerical CFD code in order to calculate the flow in a cavity with length scales of about 2 m. As a result of his simulations he described the existence of a relatively stagnant zone in the upper part of the cavity, in which the hot air is stratified. Another model for the convective heat losses was proposed by Clausing [6]. The shear layer between the stratified stagnant air in the upper zone and the cold air in the lower, so called convective zone, was treated like a wall. In the model the heat fluxes of the inner walls and the shear layer are calculated with correlations for a flat plate. The energy transport from the convective zone through the aperture was modeled with a simple approach for a buoyant flow. Altogether the set of equations can be solved in order to estimate the convective heat losses.

Besides modeling, some experimental studies were conducted. In [11] the results of an experiment with an electrically heated cubic cavity with an inner length of 2.2 m are presented. On side of the cube was opened. The convective heat losses and velocity and temperature profiles in the aperture plane were measured for different wall temperatures of this horizontal cavity. The results of a heat loss analysis for a 5 MW_{th} receiver at the top of a power tower has been presented in [14].

Some other analyses were performed with small scale receivers. In order to keep reach the high Rayleigh-numbers of real scale receivers and therefore to analyze a comparable flow, Hess [10] conducted an experiment with an electrically heated cavity in water. Clausing performed an experiment with an electrically heated cavity in a cryogenic wind tunnel [7]. The walls of a cubical cavity were heated up to a specific temperature, the heating was stopped and the cooling rates of the different cavity walls were measured. From these cooling rates the heat transfer coefficient for the different walls were obtained. In this experiment, different aperture sizes and positions were analyzed. The results supported the assumption made in [6] that the walls in the stagnant zones are adiabatic. In [9] the performance of a cavity receiver similar to the CESA-1 receiver was analyzed using a Monte-Carlo method for the radiation and the convective losses were calculated with a CFD code. The influence of wind on the convective losses was also simulated. The temperature in the cavity does not change very much with increasing wind speed as it was predicted in [6]. However the heat losses change significantly, which the authors explained with the increased wind speed inside the cavity.

Many more studies were performed to analyze the convective heat losses of cavity receivers for solar dish systems. These cavities are smaller and therefore easier to handle in an experiment. The losses of the receiver for the Solar Total Energy Project caused by natural convection were analyzed in [16]. Afterwards the effect of wind on the heat losses of the same receiver was analyzed in [13]. Two different types of spherical receivers were analyzed in [12]. A comparison between a CFD analysis of the convective losses and an experiment are presented in [15] for a very small electrically heated model receiver with an inner diameter of 70 mm. Simulation and experimentation were in good agreement, showing that it is possible to predict the convective heat losses using CFD, at least for small receivers.

3.2. Estimation of heat loss using correlations

To estimate the heat transfer coefficient for the thermal model, several correlations given by the above mentioned literature were analyzed. The heat transfer coefficient was therefore evaluated for the specific cavity dimensions and inclination angle for several average cavity temperatures. As it can be seen in the diagram (Fig. 4) the correlations show a wide range of results for the heat transfer coefficient (results are shown for design V1). The correlation given in [12] was used to evaluate the heat transfer coefficient at an average cavity temperature of 800°C. Within the thermal simulations a heat transfer coefficient of 3.5W/m^{2}K for V1 and 2.5W/m^{2}K for V2 was modeled. The forced convection boundary was considered on the complete inside of the cavity using the ambient temperature as bulk temperature. The effect of the stagnation zone was neglected because of complexity and uncertainties of the real position and size of the stagnation zone.

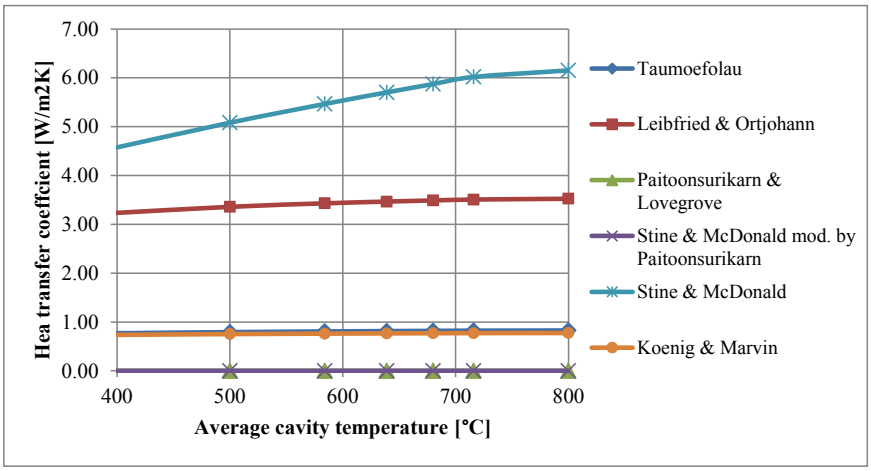

Fig. 4: Heat transfer coefficient using correlations

3.3. CFD Model

The results of the thermal model showed that high heat losses by convection are expected at the receiver. Further the correlations showed a wide range in results. Finally all correlations are not validated for the receiver sizes presented in the paper. Another point is that all these correlations are evaluated for smooth cavity walls without considering absorber tubes. The proposed receiver design instead uses absorber tubes arranged with a specific spacing to reduce thermal gradients in the tube walls by internal reflections. This additional area must have an influence on the heat transfer and will increase the heat transfer. Last but not least, the temperature within the cavity will be not homogenous as it was assumed in the correlations.

Therefore a CFD model was used to analyze the heat losses considering the geometry of the absorber tubes and the thermal field given by the thermal models. The air in the receiver and part of the ambient air were modeled. Using the symmetry effect, the model is halved to reduce computational time. The geometry was meshed using tetrahedrons and prism layers for resolving the boundary layer. The near wall mesh was refined until an average value of one for the dimensionless wall distance (y^+) was reached to ensure correct heat transfer calculation between wall and fluid. The SST turbulence model was used for steady state and transient simulations. The cavity and absorber tube walls were modeled with a fixed thermal boundary representing the temperature distribution (from thermal FE model). The simulations were performed for several load situations to analyze the effect of the part load situation.

3.4. Results of the CFD analysis

The CFD simulations showed that the heat losses are much higher than they were expected by the correlations. Therefore the receiver efficiency will be lower than estimated using the correlation.

The main reason behind the higher losses is the additional area of the absorber tubes. It was found that the heat losses are about two times higher for all analyzed temperature distributions (including part load cases of the receiver). The heat transfer coefficient was determined to be between 8 and 10W/m^{2}K.

Consequently the heat losses for the presented receiver designs will be much higher than expected and therefore the receiver efficiency lower. The efficiency of receiver V1 for example is reduced from 75% to 67% at design point conditions without wind. Fig. 5 shows the CFD model and some typical results showing the convective losses by cold air entering the receiver at the bottom and hot air leaving the receiver at the top.

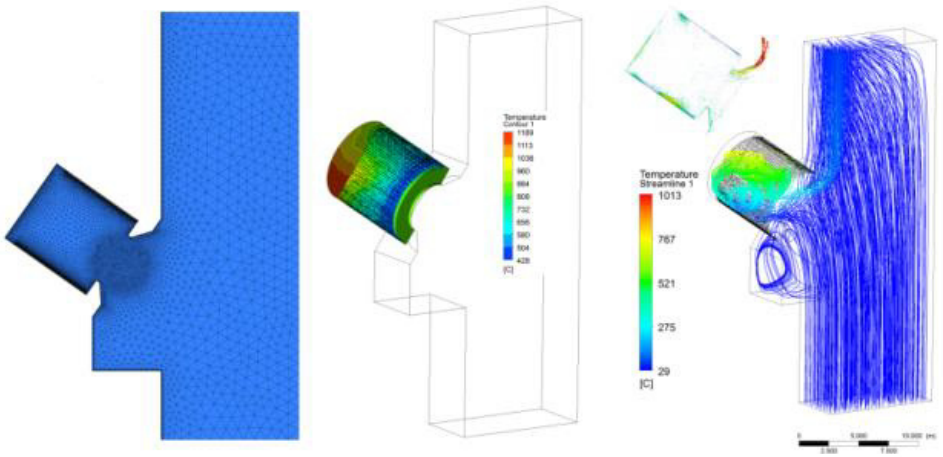

Fig. 5: CFD model (mesh, temperature distribution, fluid flow)

The results of the transient simulations under wind conditions showed a wide range of results. In some wind situations the heat losses are increasing while other wind directions (strong wind from side) could reduce the convection losses drastically. Reason for this is that the inflow and outflow of the air across the aperture is blocked. Currently these CFD results are not validated by experiments. Therefore the already used correlation [12] was used for evaluating the heat losses of the studied receiver designs. In any case the convection losses are much too high for such a system. Hence focus is aligned on strategies to reduce these losses.

4. Strategies to enhance receiver efficiency

Several possible solutions to reduce the convection losses can be imagined. The following list tries to give an overview on them:

- Increasing receiver dimension but keeping aperture constant (here shown as V1 and V2).
- Reducing the aperture by using a secondary concentrator.
- Increasing the receiver inclination angle (“face down”).
- Adding an additional geometry (cone) to disturb the inflow and outflow of ambient air into the receiver.
- Using a wind curtain to disturb or block the inflow and outflow of ambient air into the receiver.
- Covering (full/partly) the aperture by using a transparent material (here shown as V1w, see Fig. 6).

Due to the good results in former projects this paper deals with the impact of using a transparent covering to reduce the convection. Consequently this does not mean that the other options are not worth investigation. This will be done in future work.

5. Transparent covering of aperture

5.1. Design

Fused silica has a very high solar transmissivity, but a low transmissivity for longer wavelengths. Additionally, the very low thermal expansion coefficient leads to a high tolerance to temperature gradients in the material. Therefore, this material is well suited for use as a transparent covering of the receiver aperture. Within the ARTRANS project [21] such a window was designed and successfully tested. The prototype with an area of approximately 1m^2 was covered with a broadband antireflective coating. The coating was realized by a porous silica single layer with a quarter wavelength thickness [21].

The proposed design of a window for the receiver (V1) follows the same approach. 18 segments of halved fused silica tubes with an outer diameter of 197mm, a wall thickness of 9mm and a maximum length of 4.5m are bedded in a support frame of insulation material. Between the segments a small gap of about 10mm is foreseen to avoid touching the segments themselves and to reduce manufacturing accuracy. Fig. 6 shows a sketch of the proposed segmented receiver window.

Fig. 6: Receiver design V1w with segmented window

5.2. Modeling semitransparent properties of fused silica

The optical properties of fused silica are advantageous for use in solar receivers. It provides a high transmissivity in the solar radiation band (wavelength < about 2E-6 m) and lower transmissivity for thermal radiation. That means that using fused silica not only reduces the convective losses, it also reduces the radiation loses as the infrared radiation is partly reflected and absorbed within the glass. The higher temperature of the glass leads to thermal radiation in both directions (ambient and absorber side).

The radiation properties of the glass depend strongly on the material [18]. For modeling the solar radiation it can be useful to divide the radiation spectrum into discrete number of wavelength bands [19].

The effect of a glass window on the thermal re-radiation out of the receiver cavity was evaluated with a very simple model. The thermal radiation of the walls was assumed to be homogeneous. At different temperatures (600 K , 800 K, 1000 K and 1200 K) the black body radiation from the walls was calculated. The Surroundings were also assumed to be uniform in temperature (300 K). These considerations lead to values for the net thermal radiation from the hot walls. For the case with absorption of thermal radiation in the glass, the semi-transparent properties of the glass have been taken into account. In Fig. 7 the schematic of the simple model is shown. On the left side the case considering thermal radiation without a window is shown, on the right side the case with glass is shown.

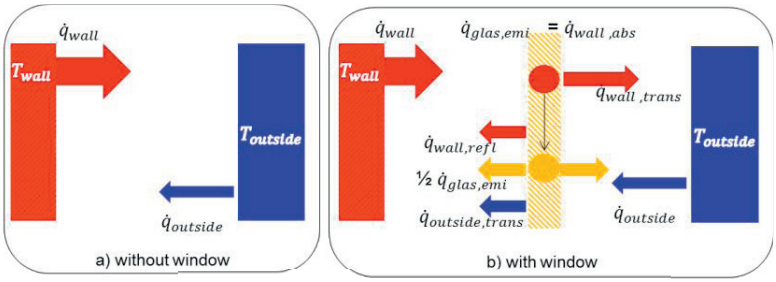

Fig. 7: Schematic of the simple physical model

5.3. Reduction of thermal losses

The reduction of the thermal losses was calculated using the reduction factor estimated by the simplified physical model. The heat losses by convection to ambient for the window itself were estimated using a correlation for free convection of a hot plate [4]. Conduction loss to the support frame was neglected due to the small contribution to the overall loss. The convection losses of the cavity were set to zero. Even if a broadband anti-reflective coating increases the transmissivity from 97% up to 99% additional reflection losses of 3% were assumed due to possible pollution of the window. As it can be seen in Fig. 7 the receiver efficiency is dramatically increased.

At the design point the efficiency increased up to 83%. Furthermore the semi-transparent behavior of the fused silica blocks the thermal radiation at lower temperatures (part load) of the receiver and therefore the efficiency is not reduced as much as in receiver designs without a window. It must be clear that such optical systems have to be cleaned regularly (daily) not only to ensure high transmissivity, but more importantly to prevent dirt reacting with the glass material. A cleaning could be accomplished using pressurized water to clean the window automatically.

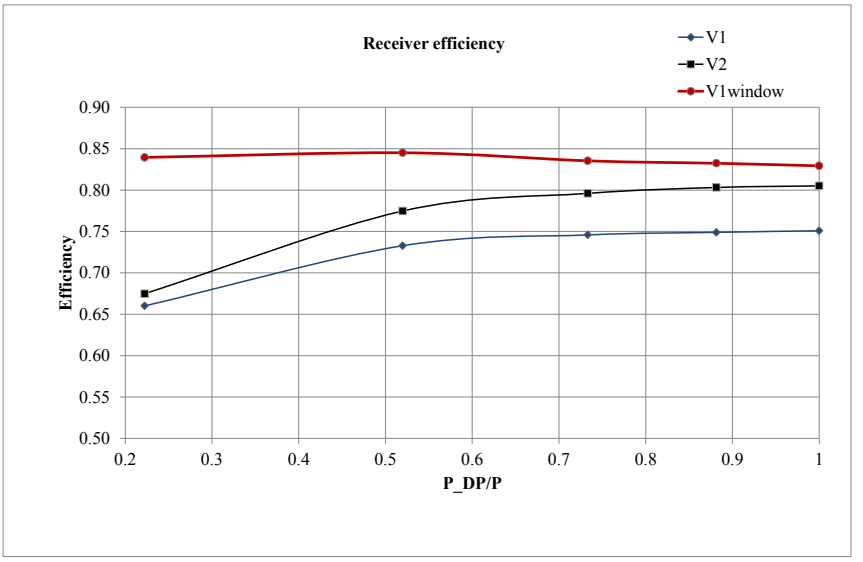

Fig. 8: Receiver efficiency (including window)

6. System modeling

To analyze the impact of the different receiver designs a solar-hybrid combined cycle (SHCC®) power plant using the performance and cost data of the receivers has been modeled and analyzed in terms of annual yields and levelized cost of electricity (LCOE). Fig. 1 shows a typical flow schematic. Regarding the technical and economical results the SHCC plants were compared with a conventional fossil-fired combined cycle working at base-load (24h) and solar only (SO) operation. The power plants in this study were operated at full-load and no specific load characteristics were considered. To analyze the influence of different receiver design options on the LCOE, performance calculations on an annual basis were done. All concepts were compared in terms of solar share, fossil fuel consumption and plant efficiencies. The methodology for system simulation and economic assessment used in this study is similar to reference [22]. The layout and cost optimization of the solar fields including the receiver was done with HFLCal software [24]. Thermal heat balance calculations, simulation and annual performance calculation was completed using the commercial software EBSILON®. An EXCEL®-interface enables the calculation of solar-hybrid power plants over a full year, considering hourly values of solar irradiation (DNI), weather conditions, solar position angles and operation strategy.

The SHCC power plants were designed and modeled for the site Sanlúcar la Mayor in Spain with a total net power of 6.2 MW_e. The solarized gas turbine (SolarTurbines® MERCURY 50) provides about 3.9 MW_e at design point conditions and the bottoming steam cycle 2.3 MW_e at design point. The system contains a single pressure heat recovery steam generator and has dry cooling. The total power block gross efficiency is about 38.7 % at design point.

All solar fields have a solar multiple of 1, providing the required receiver design thermal power of 8.4 MW_{th} to heat the pressurized air from 330 °C to 800 °C (in this study, no thermal storage was used). To match the turbine inlet temperature of about 1170°C and provide constant turbine inlet conditions despite fluctuating solar input a combustion chamber heats the air before entering the gas turbine.

Table 3: Investment cost input and financial boundary conditions

Parameter	Unit	Value
Direct investment costs		
Spec. cost solar field	[€/m²]	140
Spec. cost receiver (low / high / high+ efficiency)	[€/kWth]	135 / 225 / 147
Spec. cost tower (K1 = 375000 €, H1 = 11.07 €/m, TVER = tower height, ALPHA = 2.392) [5]	[€]	$C_{tower}[€] = K1 + H1 \times TVER^{ALPHA}$
Spec. cost power block (Reference / SHCC incl. solarization)	[€/kWe]	~ 702 / ~ 916
Spec. cost land	[€/m^2]	3
Indirect costs (used for all systems)		
surcharges for construction, engineering and risks	[%]	30, as percentage of total direct cost
Financing parameters		
Interest rate	[%]	8
Life time	[a]	25
O&M		
Insurance, equipment, escalation	[% of EPC]	3
Fuel cost	[€/MWh]	30
Total plant cost incl. owners cost (V1 / V2 / V1w)	[M€]	~13.4 / ~14.1 / ~13.2
Specific investment (V1 / V2 / V1w)	[€/kWe]	2,14 / 2,25 / 2,10

The LCOE were calculated according to a simplified IEA method [25]. To calculate the solar LCOE† for plants with solar-only operation a second reference plant with equal capacity and operational hours was considered.

The results of the annual performance calculation show that hybrid-plants working in base-load operation have lower LCOE than plants working at solar-only. In contrast, plants in solar-only operation show higher solar LCOE, caused by fewer operational hours but at the same amount of investment cost. Comparing the systems with low efficiency receivers (V1) against systems with high efficiency receivers (V2) the results show that the LCOE are lower for V1 although the efficiencies for V2 are higher. The reason for this is that the investment costs for V2 are considerably higher. The introduction of the window (V1w) shows an overall positive effect: the efficiencies are increased and the LCOE are the lowest compared to the other systems.

SHCC plants that are operating in solar-only mode show higher annual solar share‡ (up to 31.1% for V1-SO, see Fig. 10) than plants operating around the clock (V1-24h, V2-24h & V1w-24h with a maximum of 11.1%). The latter have a higher demand for fossil firing. The plant with high receiver efficiency (V1w-SO) has the lowest solar share of the plants operated in solar-only mode. The reason for this is a higher fuel demand, which is caused by an increase in operation hours even at low solar irradiation.

† $LCOE_{(solar)}=(LCOE_{total}*W_{el}-LCOE_{ref}*Q_{fuel}*eta_{ref})/(W_{el}-Q_{fuel}*eta_{ref})$ [23]

‡ The solar share is defined as a ratio of solar thermal input over total thermal input.

Table 4: Technical specifications and results @DP

Technical specifications @DP	**Reference**	**SHCC**	**SHCC**	**SHCC**
Receiver	-	V1	V2	V1w
Solar multiple	0	1	1	1
Storage capacity	0 h	0 h	0 h	0 h
Flux (mean, incident)	-	730 kW/m²	725 kW/m²	805 kW/m²
HTF	Air	Air	Air	Air
Receiver temperature	-	335 °C – 800 °C	335 °C – 800 °C	335 °C – 800 °C
Solar field size	0 m²	18448 m²	16982 m²	16982 m²
Fossil thermal power	16.97 MW_{th}	7.83 MW_{th}	7.83 MW_{th}	7.83 MW_{th}
Therm. power receiver	0 MW_{th}	8.4 MW_{th}	8.4 MW_{th}	8.4 MW_{th}
Nominal gross power	6.7 MW_{el}	6.3 MW_{el}	6.3 MW_{el}	6.3 MW_{el}
TIT	1170 °C	1170 °C	1170 °C	1170 °C
Steam conditions ST	450°C @ 30 bar	450°C @ 30 bar	450°C @ 30 bar	450°C @ 30 bar
Exhaust ST	60°C @ 0.15 bar	60°C @ 0.15 bar	60°C @ 0.15 bar	60°C @ 0.15 bar
$\eta_{PB,\ electrical\ gross}$ @DP	39.7%	38.3%	38.3%	38.3%
η_{field} @DP	-	73.9%	74.3%	73.8%
$\eta_{receiver}$ @DP	-	75.3%	80.9%	82.9%
$\eta_{el,\ gross\ plant}$ @DP	39.7%	27.3%	28.8%	29.1%
solar share @DP	-	51.8%	51.8%	51.8%

Table 5: LCOE and LCOE (solar) of all configurations with base-load (24h) and solar only operation (SO)

LCOE [€/kWh]	V1-24h	V2-24h	V1w-24h	V1-SO	V2-SO	V1w-SO
LCOE Reference	0.088	0.088	0.088	0.132	0.132	0.118
LCOE	0.096	0.098	0.096	0.166	0.171	0.142
LCOE (solar)	0.176	0.196	0.169	0.274	0.293	0.243

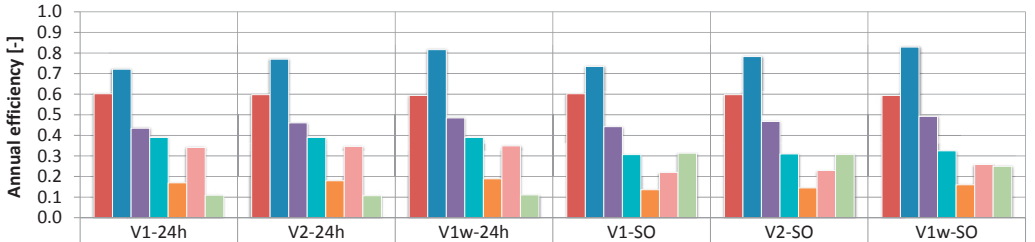

	V1-24h	V2-24h	V1w-24h	V1-SO	V2-SO	V1w-SO
eta field	0.602	0.598	0.594	0.602	0.598	0.594
eta rec	0.722	0.770	0.816	0.735	0.783	0.829
eta solar	0.434	0.460	0.485	0.442	0.468	0.492
eta PB net (solar + fossil)	0.390	0.390	0.390	0.306	0.309	0.325
eta total net (solar)	0.169	0.179	0.189	0.135	0.145	0.160
eta total net (solar + fossil)	0.341	0.346	0.349	0.220	0.229	0.258
solar share	0.109	0.107	0.111	0.313	0.307	0.250

Fig. 9: Annual efficiency of all configurations with base-load and solar only operation (Reference-24h: eta_PB_net = 0.369, Reference-SO-V1&V2: eta_PB_net = 0.339, Reference-SO -V1w: eta_PB_net = 0.351)

7. Conclusions

The limited heat transfer of gaseous flows lead to large absorber areas for metallic tubular receivers. Increasing the receiver size helps to reduce the heat flux and therefore lowers the temperatures of the receiver. Following the losses mainly by radiation to ambient are reduced. But this approach increases the specific receiver costs in the same way. Another possible strategy to reduce the convection losses is a transparent window covering of the aperture. A design of such a window was proposed and the reduced losses were analyzed. A CFD model was used to analyze the convection losses in addition to given correlations by literature. The thermal model of the three receiver designs showed receiver efficiencies at design point conditions of 75% for a small, 80% for a large and 83% for a small receiver with window. Finally the three receiver designs were compared on LCOE base in a system study. The results show that a larger receiver does not lead to lower electricity costs as the specific costs are higher and so do not justify the higher costs. The proposed usage of a window instead showed a significant reduction of electricity costs. Future work should study this concept more in detail and in the same way the other proposed strategies.

Acknowledgements

The support from the German Federal Environment Ministry (BMU) (Contract No. 0325221B) is gratefully acknowledged.

References

[1] C. Sugerman, A.Ring, R.Buck, P.Heller, Solar-hybrid gas turbine power plants – test results and market perspective (ISES2003)
[2] L.Amsbeck, R.Buck, P.Heller, J.Jedamski, R.Uhlig Development of a tube receiver for a solar hybrid microturbine system, Solarpaces 2008, March 4-7, Las Vegas, USA
[3] Roman Korzynietz, Manuel Quero, Ralf Uhlig SOLUGAS – Future solar hybrid technology, Solarpaces 2012, Marrakech, Marocco
[4] Verein Deutscher Ingenieure: VDI-Wärmeatlas, 10. Aufl. Springer-Verlag, Berlin, 2006.
[5] Verband der Technischen Überwachungs-Vereine e. V.: AD 2000 – Regelwerk, Carl Heymanns Verlag KG, Taschenbuch Ausgabe 2003.
[6] Clausing, A. M. (1981): An Analysis of Convective Losses from Cavity Solar Central Receivers. In: Sol. Energy 27 (4), S. 295–300.
[7] Clausing, A. M.; Waldvogel, J. M.; Lister, L. D. (1987): Natural Convection From Isothermal Cubical Cavities With a Variety of Side-Facing Apertures. In: J. Heat Transfer 109 (2), S. 407.
[8] Eyler, L. L. (1979): Predictions of convective losses from a solar cavity receiver. Battelle Pacific Northwest Labs., Richland, WA (USA).
[9] Fang, J. B.; Wei, J. J.; Dong, X. W.; Wang, Y. S. (2011): Thermal performance simulation of a solar cavity receiver under windy conditions. In: Sol. Energy 85 (1), S. 126–138.
[10] Hess, C. F.; Henze, R. H. (1984): Experimental Investigation of Natural Convection Losses From Open Cavities. In: Journal of Heat Transfer 106 (2), S. 333–338.
[11] Kraabel, J.S (Hg.) (1983): An Experimental Investigation of the Natural Convection from a Side-Facing Cubical Cavity.
[12] Leibfried, U.; Ortjohann, J. (1995): Convective Heat Loss from Upward and Downward-Facing Cavity Solar Receiver: Measurements and Calculations. In: Journal of solar energy engineering-transactions of the ASME 117 (2), S. 75–84.
[13] Ma, R.Y (1993): Wind effects on convective heat loss from a cavity receiver for a parabolic concentrating solar collector. Sandia National Labs., Albuquerque, NM (United States); California State Polytechnic Univ., Pomona, CA (United States). Dept. of Mechanical Engineering (SAND--92-7293).
[14] MCMORDIE, R. K. (1984): Convection heat-loss from a cavity receiver. In journal of solar energy engineering-transactions of the ASME 106 (1), S. 98–100.
[15] Paitoonsurikarn, S.; Lovegrove, K.; Hughes, G.; Pye, J. (2011): Numerical Investigation of Natural Convection Loss From Cavity Receivers in Solar Dish Applications. In: J. Sol. Energy Eng. Trans.-ASME 133 (2), S. 10.
[16] Stine, W.B; McDonald, C.G (1989): Cavity receiver heat loss measurements. In: ISES World Congress. ISES World Congress. Kobe, Japan.
[17] Tracey, T. R.; Blake, F. A.; Royere, C.; Brown, C. T. (1977): One MWth solar cavity steam generator solar test program. In: C. Beach und E. Fordyce (Hg.): International Solar Energy Society, Annual Meeting, S. 21.
[18] Wu, Y. C.; Wen, L. C. (1978): Solar Thermal Power Systems Advanced Solar Thermal Technology Project: Solar receiver performance in the temperature range of 300 to 1300/sup 0/C. Jet Propulsion Lab., Pasadena, CA (USA).
[19] Manara, et al.: Determination of the Complex Refractive Index of Glass. Report ZAE 2-1000-5 (2004), ZAE, Bayern, Würzburg 2005
[20] Röger: Fensterkühlung für solare Hochtemperatur-Receiver. PhD Thesis, DLR Stuttgart, Germany, 2005.
[21] Uhlig et al.: Development of a Broadband Antireflection Coated Transparent Silica Window for a Solar-Hybrid Microturbine System, Solar Paces 2009
[22] Giuliano, S., Buck, R., Eguiguren, S., Analysis of Solar-Thermal Power Plants With Thermal Energy Storage and Solar-Hybriod Operation Strategy, Journal of Solar Energy Engineering, Vol. 133, ASME, 2011
[23] Giuliano, S., Schillings, C., Hoyer-Klick, C., Al Nuaimi, S., Al Obaidli, A., USHYNE – Upscaling of solar-hybrid gas turbine cogeneration units, Final Report, 2008

[24] Schwarzbözl, P., Schmitz, M., Pitz-Paal, R., Visual HFLCal – A Software Tool for Layout and Optimization of Heliostat Fields, 15th International SolarPACES Symposium, Berlin, 2009
[25] Montebello C., Guidelines for the Economic Analysis of Renewable Energy Technology Applications, International Energy Agency, OECD Publications, Paris, 1991